



Synoptic weather patterns for large wildfires in the northwestern United States—a climatological analysis using three classification methods

Shiyuan Zhong¹ · Lejiang Yu² · Warren E. Heilman³ · Xindi Bian³ · Hannah Fromm¹

Received: 18 September 2019 / Accepted: 20 April 2020 / Published online: 23 May 2020

© This is a U.S. government work and not under copyright protection in the U.S.; foreign copyright protection may apply 2020

Abstract

Wildfire regimes respond to atmospheric variability on multiple time scales from interannual variations of drought to daily fluctuations of humidity and wind. Synoptic weather patterns effectively link both short- and long-term atmospheric variability, and thus, understanding fire-prone synoptic patterns is an integral part of fire management programs. Different analysis procedures of varying complexity have been used to identify the most common synoptic weather patterns conducive to wildfires. In this study, we examine the utility of three synoptic-pattern classification methodologies, namely Composite, Empirical Orthogonal Function (EOF), and Self Organizing Map (SOM). We focused on the synoptic weather patterns associated with 203 wildfires that burned 50,000 acres (20,250 ha) or more and 80 wildfires that burned 100,000 acres (40,500 ha) or more in the Northwestern United States between 1984 and 2014. The basic 500-hPa geopotential height patterns identified by the three analysis methods were found to be similar for the two fire-size categories, but the strengths of the geopotential height anomalies were larger for the larger size fires. All three methods were able to consistently identify the dominant pattern with only small differences in strength and position of the anomalies, but the EOF and SOM methods yielded other less dominant, but still important, patterns. Particularly, the SOM method captured transitional synoptic patterns that may account for 20–30% of these large wildfires.

Keywords Fire weather · Wildfires · Synoptic patterns · Weather typing

1 Introduction

The occurrences of large wildfires depend on several factors such as fuel, topography, and weather, and among them, weather is the most dynamic factor that can change rapidly and significantly during the course of a fire. Many studies have shown how weather conditions contribute to the start, spread, and duration of wildfires and to the area burned by wildfires (Bessie and Johnson 1995; Burgan et al. 1997;

Flannigan and Wotton 2001; Westerling et al. 2006; Pereira et al. 2005; Hayasaka et al. 2016). While local meteorological conditions and their fluctuations directly affect fire behavior, large-scale synoptic patterns determine prevailing wind direction and strength that exert an overall control of fire spread. Synoptic weather patterns also help determine the frequency, duration, and intensity of wildfires by affecting fuel moisture and by providing an atmospheric environment under which ignition and changes in local meteorological conditions may occur. The identification of synoptic patterns associated with wildfires and the linkage of these patterns to actual fire data or fire risk, usually expressed by fire indices, have been an area of active research. Because numerical weather forecast models are more accurate in simulating large-scale synoptic conditions than small-scale local conditions, understanding fire-prone synoptic weather patterns that link both short- and long-term atmospheric variability and aggregate all atmospheric variables in simple categorizations is crucial for fire management efforts. Earlier efforts to identify synoptic weather patterns associated with large wildfires relied heavily on

✉ Shiyuan Zhong
zhongs@msu.edu

¹ Department of Geography, Environment and Spatial Sciences, Michigan State University, 673 Auditorium Rd, East Lansing, MI 48824, USA

² Polar Research Institute of China, Pudong, Shanghai, China

³ US Forest Service, Northern Research Station, Lansing, MI 48910, USA

daily weather maps and simple subjective approaches such as visualization and composites (e.g., Schroeder 1969; Newark 1975; Brotak and Reifsnyder 1977; Takle et al. 1994). Later studies took advantage of the availability of gridded analysis or reanalysis products and utilized more objective statistical methods (e.g., correlation and linear regression) and clustering techniques (e.g., standard k or c-means, Empirical Orthogonal Function, Self Organizing Maps) in their analyses (Pereira et al. 2005; Westerling et al. 2006; Crimmins 2006; Trouet et al. 2009; Hayasaka et al. 2016; Ruffault et al. 2016; Paschalidou and Kassomenos 2016; Duane and Brotons 2018).

The objective of this study is to compare three pattern classification methods, namely the Composite, Empirical Orthogonal Functions (EOF), and Self-Organizing Maps (SOM) methods, for identifying the synoptic scale weather conditions most often associated with large wildfires in the northwestern U.S. Crimmins (2006) used SOM to determine the synoptic climatology of extreme fire weather conditions over the southwestern U.S. While Crimmins (2006) and other similar studies grouped synoptic patterns based on daily fire weather indices or fire danger ratings, the current study relates actual data of large wildfires in the northwestern U.S. to their respective synoptic patterns.

The rest of the article is organized as follows. Section 2 introduces the fire data and meteorological data as well as the

three methods used in the analyses. Results are described in Section 3, starting with statistical results organized by analysis methods and ending with specific cases. The article concludes in Section 4 with implications of the main findings and future work.

2 Dataset and methods

The current study focuses on wildfires that burned large areas in the northwestern portion of the USA in a region bounded by $35^{\circ}\text{N} - 50^{\circ}\text{N}$ and $95^{\circ}\text{W} - 125^{\circ}\text{W}$ (Fig. 1). Wildfires in this region are identified using data from the Monitoring Trends in Burn Severity (MTBS) database generated by the U.S. Geological Survey and U.S. Forest Service (<http://www.mtbs.gov>). The MTBS dataset contains burn severity data, maps, and reports for all fires since 1984 that were greater than 500 acres (202.5 ha) east and 1000 acres (405 ha) west of the 100th meridian in the contiguous U.S. (Eidenshink et al. 2007). This study focuses only on very large and extremely large wildfires defined subjectively as those with burn areas exceeding 50,000 acres (20,250 ha) or 100,000 acres (40,500 ha), respectively, over the course of the fire. For the study period of 1984 through 2014, there were a total of 203 very large wildfires and 80 extremely large wildfires in the

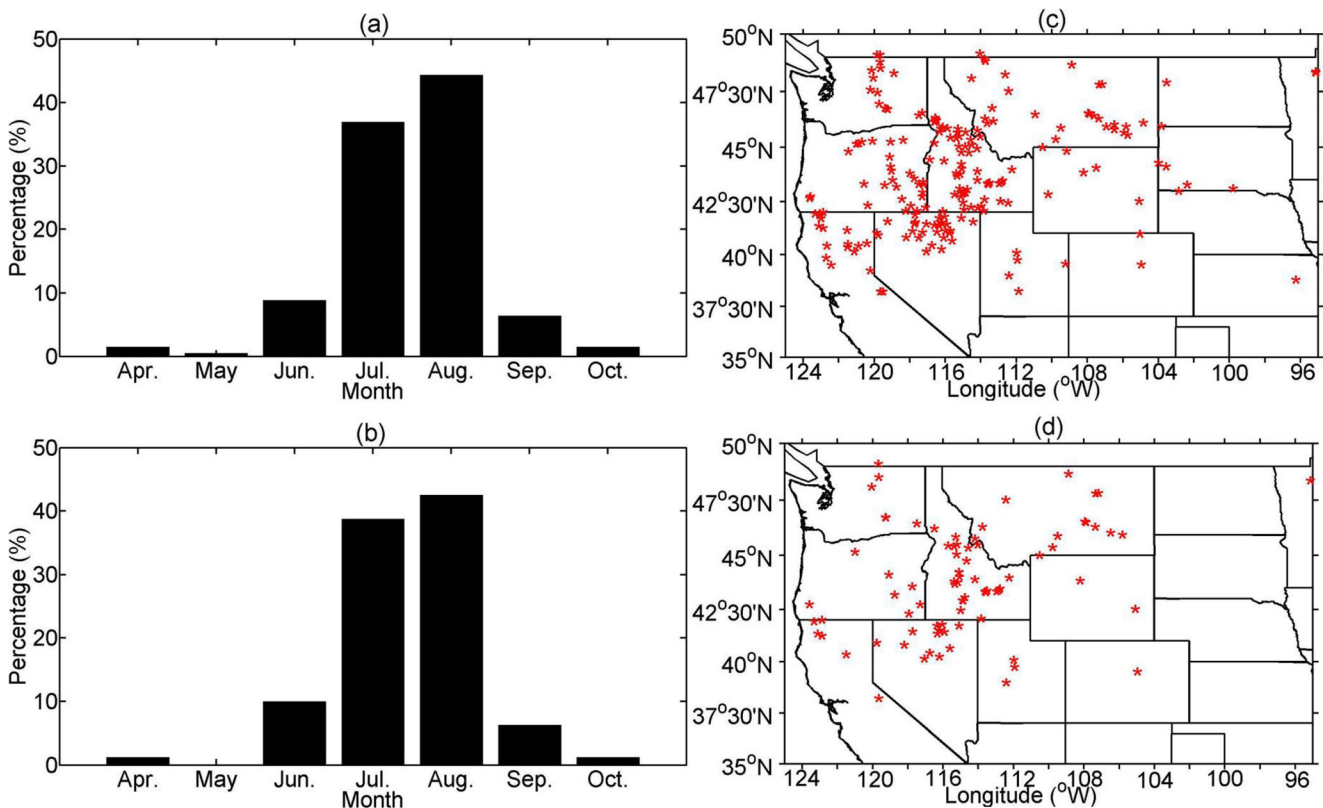


Fig. 1 The monthly percentages (a, b) and the locations (c, d) of large (a, c) or extremely large (b, d) wildfires in the northwestern U.S. that occurred during the 1984–2014 period

study domain, and the location and percentage of their occurrences in each month of the year are shown in Fig. 1.

The synoptic weather patterns corresponding to these fires are identified using data from the gridded North American Regional Reanalysis (NARR; Mesinger et al. 2006; Janjic 1994). The NARR dataset, which was generated by the National Centers for Environmental Prediction (NCEP) using the operational NCEP regional Eta model and its data assimilation system, has a horizontal resolution of 32 km at 29 pressure levels and a temporal resolution of 3-hourly from 1979 to the present. The 500-hPa geopotential height fields are extracted from NARR and utilized for synoptic circulation pattern classification because mid-latitude weather systems tend to follow winds at this pressure level. In addition, surface

air temperature, specific humidity, and wind speed are also extracted from NARR and used to characterize surface atmospheric conditions under the synoptic circulation patterns. The MTDS database contains only the starting date of each fire, and as a result, the synoptic patterns derived here reveal atmospheric conditions only at the beginning of the fires. A daily mean is first calculated from the 3-hourly NARR data, and an anomaly is computed by subtracting from the daily means the climatology for a chosen day computed by averaging daily means over the study period of 1984–2014.

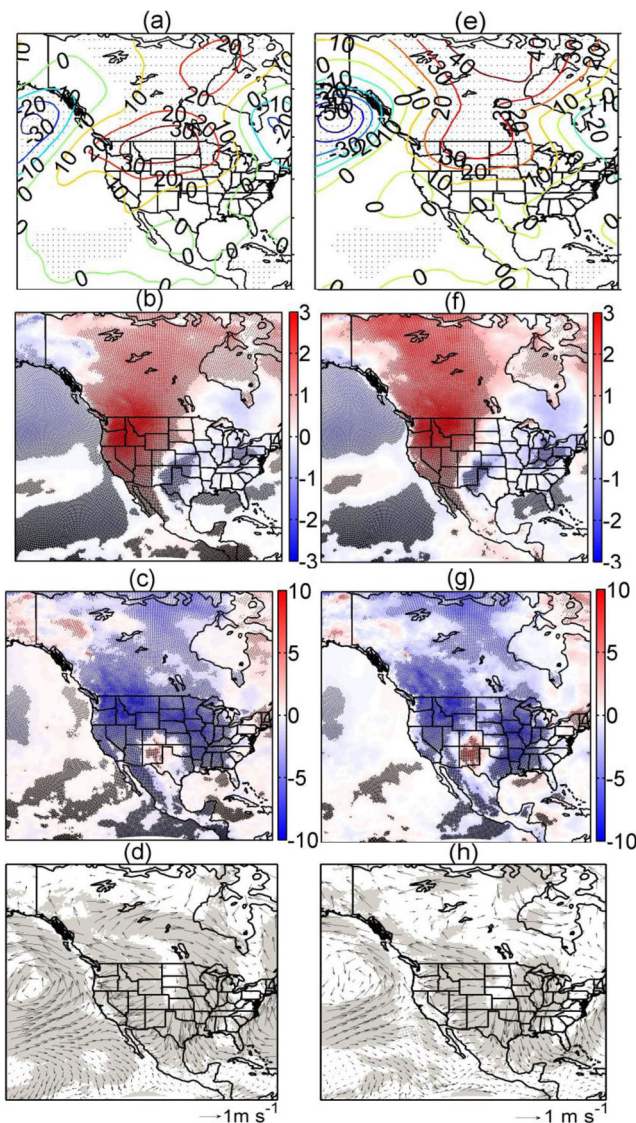


Fig. 2 Composites of the anomalies of 500-hPa geopotential height (gpm) (a, e), 2-m air temperature (°C) (b, f), 2-m relative humidity (%) (c, g) and 10-m wind field (m s^{-1}) (d, h) for very large (a–d) and extremely large (e–h) wildfires in the northwestern U.S. during the 1984–2014 period

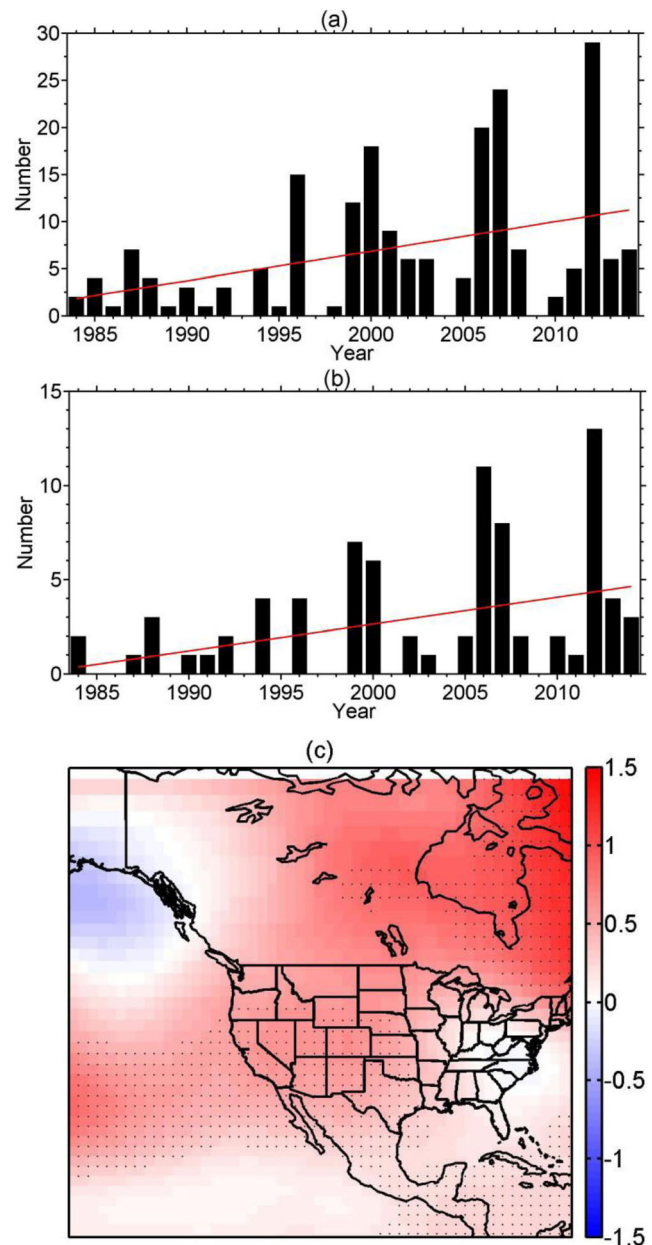


Fig. 3 Time series of the number of occurrence and linear trend (red line) of the very large wildfire events (a) and the extremely large wildfire events (b), and the composites of the June–September trends in the 500-hPa geopotential height (gpm year^{-1}) (c). The dots in c denote statistical significance above the 95% confidence level

In this study, synoptic weather patterns corresponding to the beginning of the very large or extremely large wildfires in the Northwestern US are identified using three different classification methods, namely the Composites, Empirical Orthogonal Functions (EOF), and Self-Organizing Maps (SOM).

The Composite analysis is a simple method used widely in meteorological and climatological research for identifying patterns associated with certain phenomena. It computes means and sometimes standard deviations for a set of cases collected for a chosen phenomenon. Sometimes, composites

are stratified by one or more potential factors and the results may reveal if and how the phenomenon is influenced by the factors. For this study, the Composite method is used to produce the mean patterns of the anomalous 500-hPa geopotential heights, 2-m temperatures, 2-m relative humidity, and 10-m wind speeds at the beginning of the 203 very large and 80 extremely large wildfire cases in the northwestern U.S. The statistical significance of the composite pattern is established by Student's *t* tests, using the variability within members of the composite. The advantage of the Composite

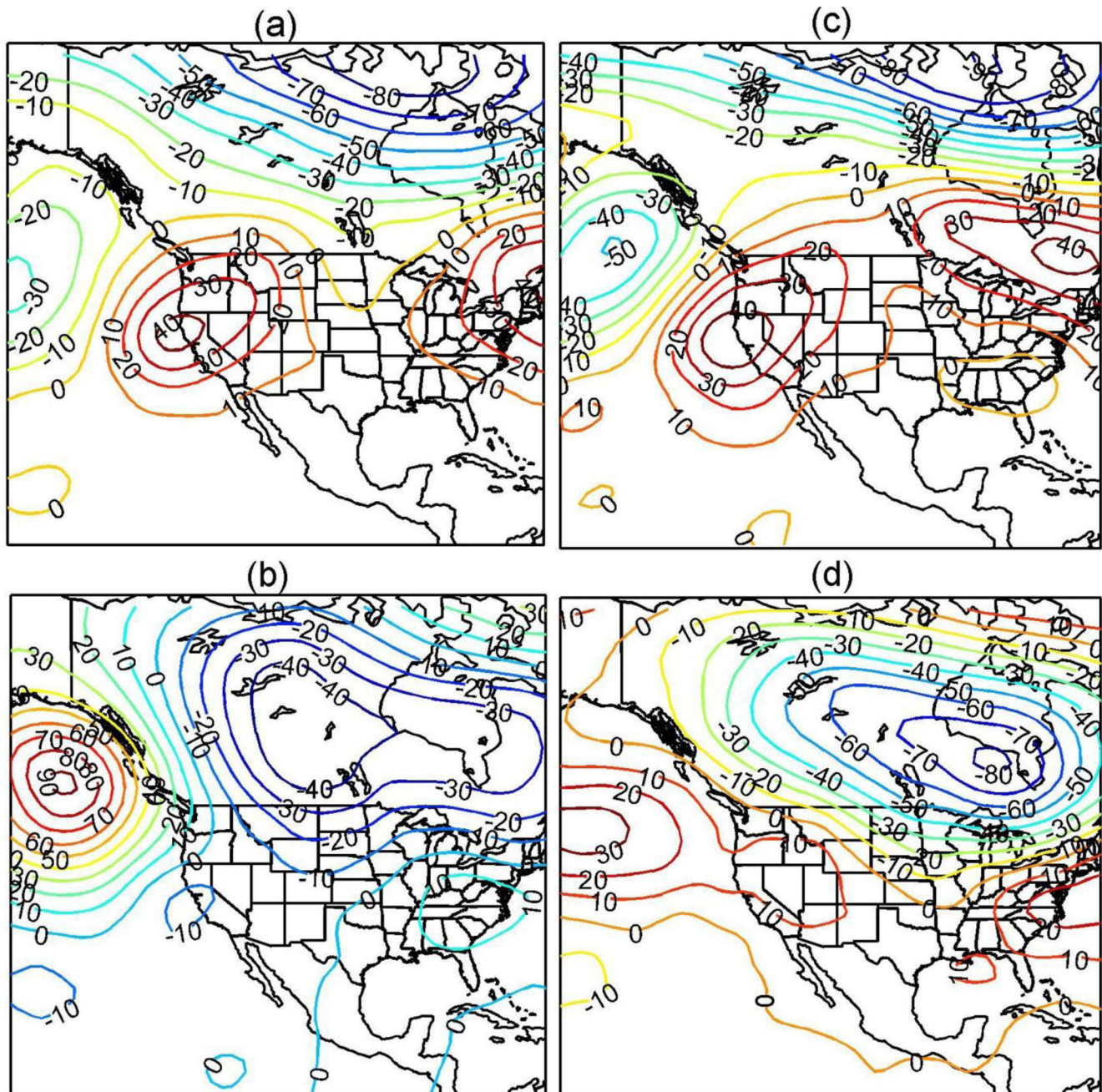


Fig. 4 Spatial patterns of the first (a, c) and second (b, d) EOF modes for the 500-hPa geopotential height anomalies (gpm) corresponding to very large wildfire events (a, b) and extreme wildfire events (c, d)

analysis lies in its simplicity. The main shortcoming is that individual features may differ somewhat in positions and strengths and averaging may lead to smeared results that may not be statistically significant.

The EOF technique (Hannachi et al. 2007) is another commonly used pattern-extraction dimension-reduction technique in weather and climate analyses. For a given dataset, the EOF technique extracts patterns or features through decomposition of the data with a set of orthogonal basis functions determined by data structure. A set of mathematically orthogonal modes is generated and is ordered based on the eigenvalues that describe the variance explained by these modes. The technique has proven powerful for identifying spatial modes of variability and how they change with time from complex weather and climate

data (e.g., Wang et al. 2017; Naren and Maity 2018). The major limitation of the EOF analysis technique is its orthogonality because physical systems, such as weather systems, are not necessarily orthogonal (Simmons et al. 1983; Monahan et al. 2009), though the use of rotated EOFs (Richman 1986) may help. Another limitation is that the EOF patterns may be domain-dependent because of the non-local requirement that the modes maximize variance over the entire domain. Thus, the results may change as the domain changes (North et al. 1982).

Since its initial introduction to meteorological and climate research in the late 1990 and early 2000 (Hewitson and Crane 2002), the SOM technique (Kohonen 1995) has been used in a variety of applications such as climate zoning (Malmgren and Winter 1999), rainfall estimation

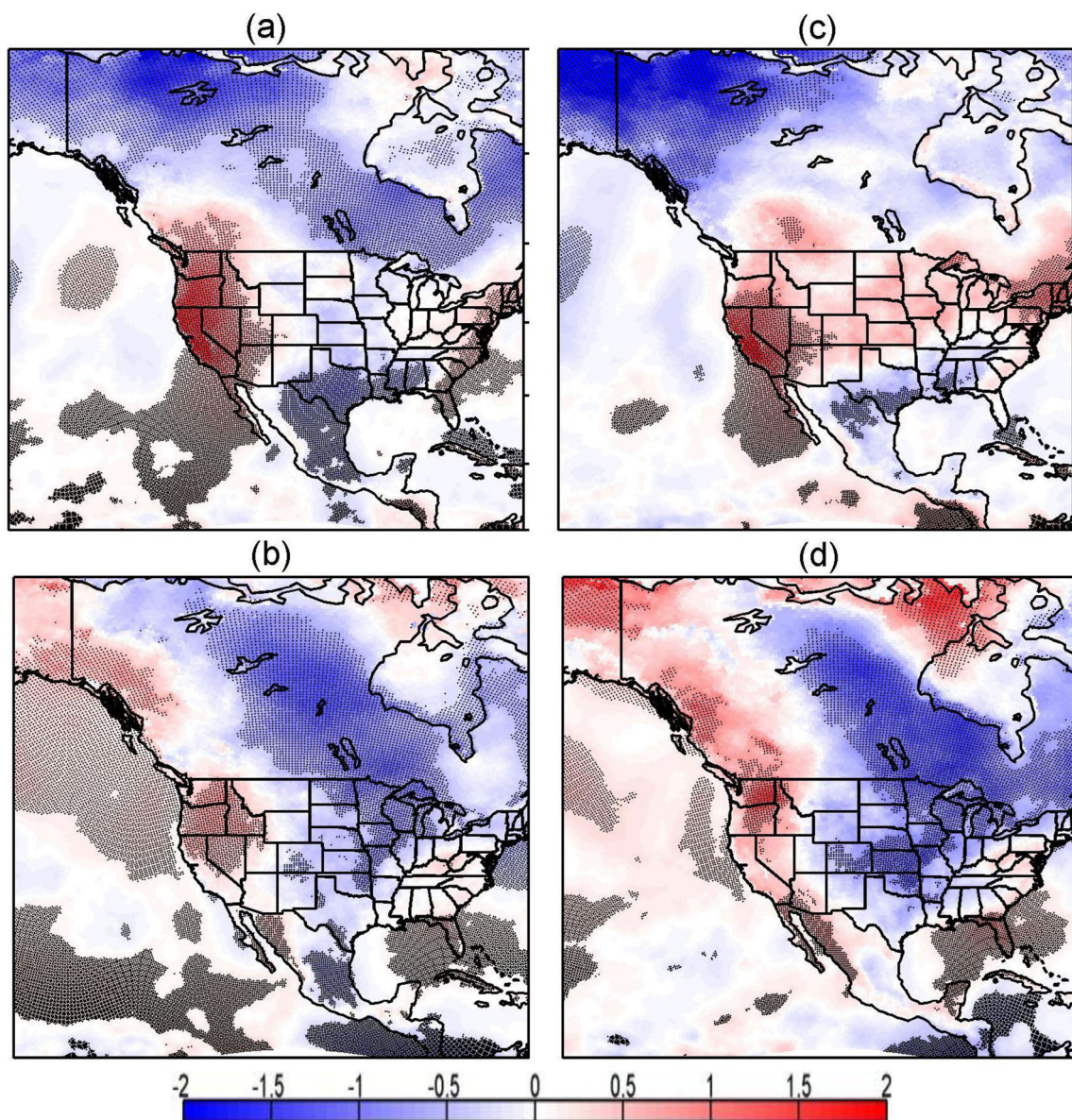


Fig. 5 The same as Fig. 4, but for 2-m air temperature anomalies (°C)

(Hong et al. 2005), and Antarctica sea-ice trend identification (Yu et al. 2018). As a type of artificial neural network, SOM transforms high-dimensional input data into a low-dimensional (usually two-dimensional) array of nodes, while preserving topographical relationships between the input data through unsupervised learning using a simple heuristic method. Unlike the EOF technique, which has difficulty identifying non-linear structures in the data, a major strength of the SOM technique is its ability to identify hidden non-linear information in high-dimensional data (Hsieh 2001). SOM results represent a continuum of synoptic patterns compared to EOF and other more traditional methods that produce discrete realizations of synoptic patterns (Sheridan and Lee 2011). Further, the SOM patterns are local in nature, which means they are not

derived by solving a global covariance matrix as required in EOF analyses (Monahan et al. 2009).

3 Results

Large wildfires in the northwestern U.S. occur predominantly in warm seasons, with summer being the peak season (Fig. 1). For very large wildfires that occurred during the 1984–2014 period, 44.3% occurred in August and 37.0% in July. The distribution is similar for extremely large fires. Although the study domain encompasses 20 states, these very large and extremely large fires occurred mostly in Montana, southern and central Idaho, eastern Washington and Oregon, and northern Nevada and California.

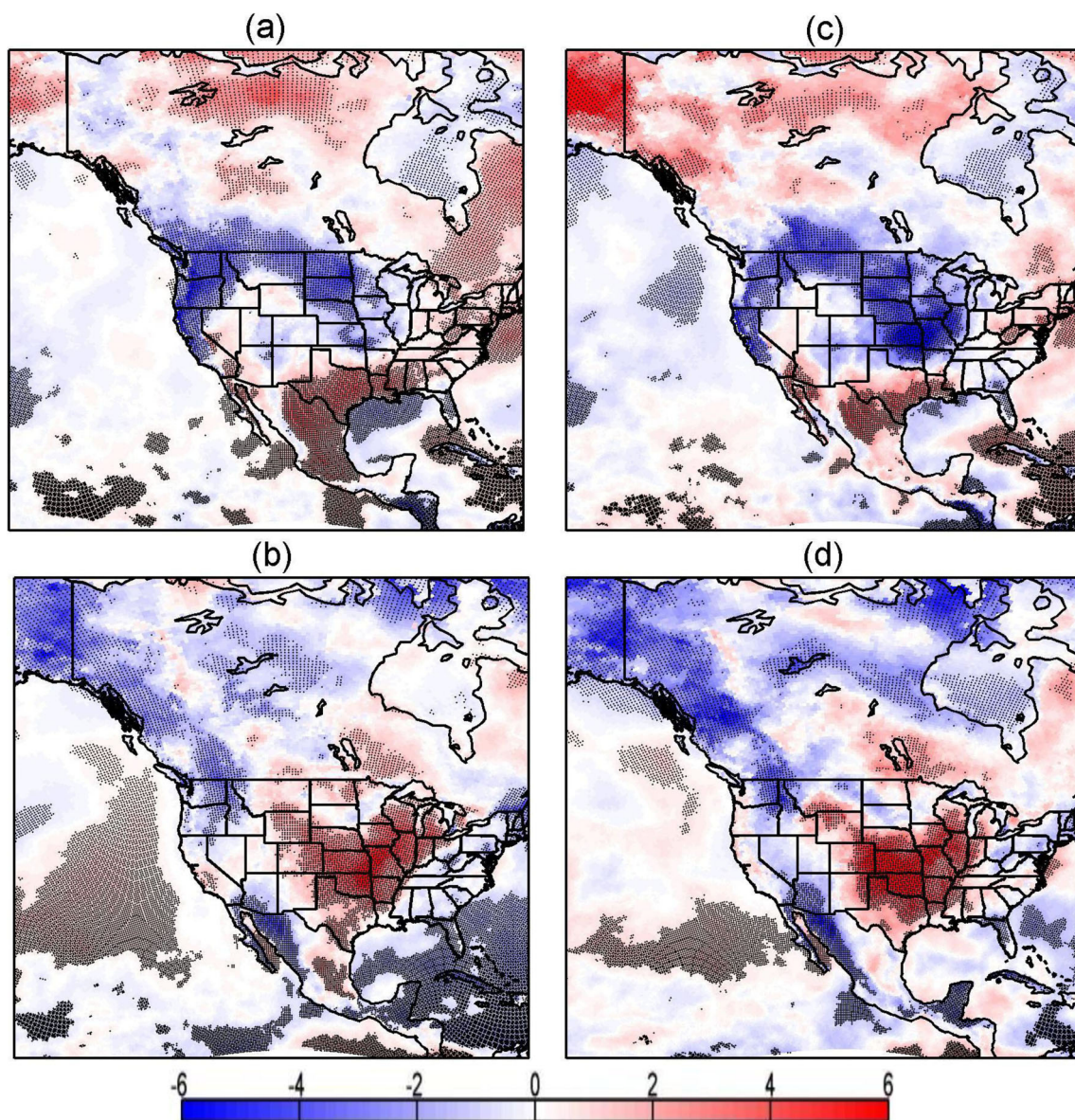


Fig. 6 The same as Fig. 4, but for 2-m relative humidity anomalies (%)

3.1 Composite analysis

Composites of anomalous 500-hPa geopotential height, 2-m air temperature, 2-m relative humidity, and 10-m wind fields are produced over the 203 very large wildfire events and the 80 extremely large wildfire events that occurred during the study period in the northwestern U.S.; the results are shown in Fig. 2. For both fire-size categories, the synoptic patterns are dominated by a blocking high with positive height anomalies over the western and central U.S. and central Canada, flanked by negative anomalies over eastern Canada and the Gulf of Alaska extending into western Canada. The spatial patterns are similar between the two fire-size categories, but there is an increase in the strength of the anomalous high in central Canada and a considerable intensification of the

anomalous low in the Gulf of Alaska going from very large to extremely large fires. At the surface, warm and dry anomalies prevail across the western U.S. and Canada, with the largest anomaly values found over the northwestern U.S. and southwestern Canada. The easterly wind branch of an anomalous anticyclonic circulation centered over the central Plains helps to bring hot and dry interior air to the western portions of the domain.

A significant (95% confidence level) upward trend is detected in the annual number of very large fires (0.31 year^{-1}) and extremely large fires (0.14 year^{-1}) over the study period of 1984–2014, although there is considerable interannual variability (Fig. 3a, b). This is consistent with the significant (above 95% confidence level) positive trend in the peak warm-season (June–September) 500-hPa geopotential height anomalies over

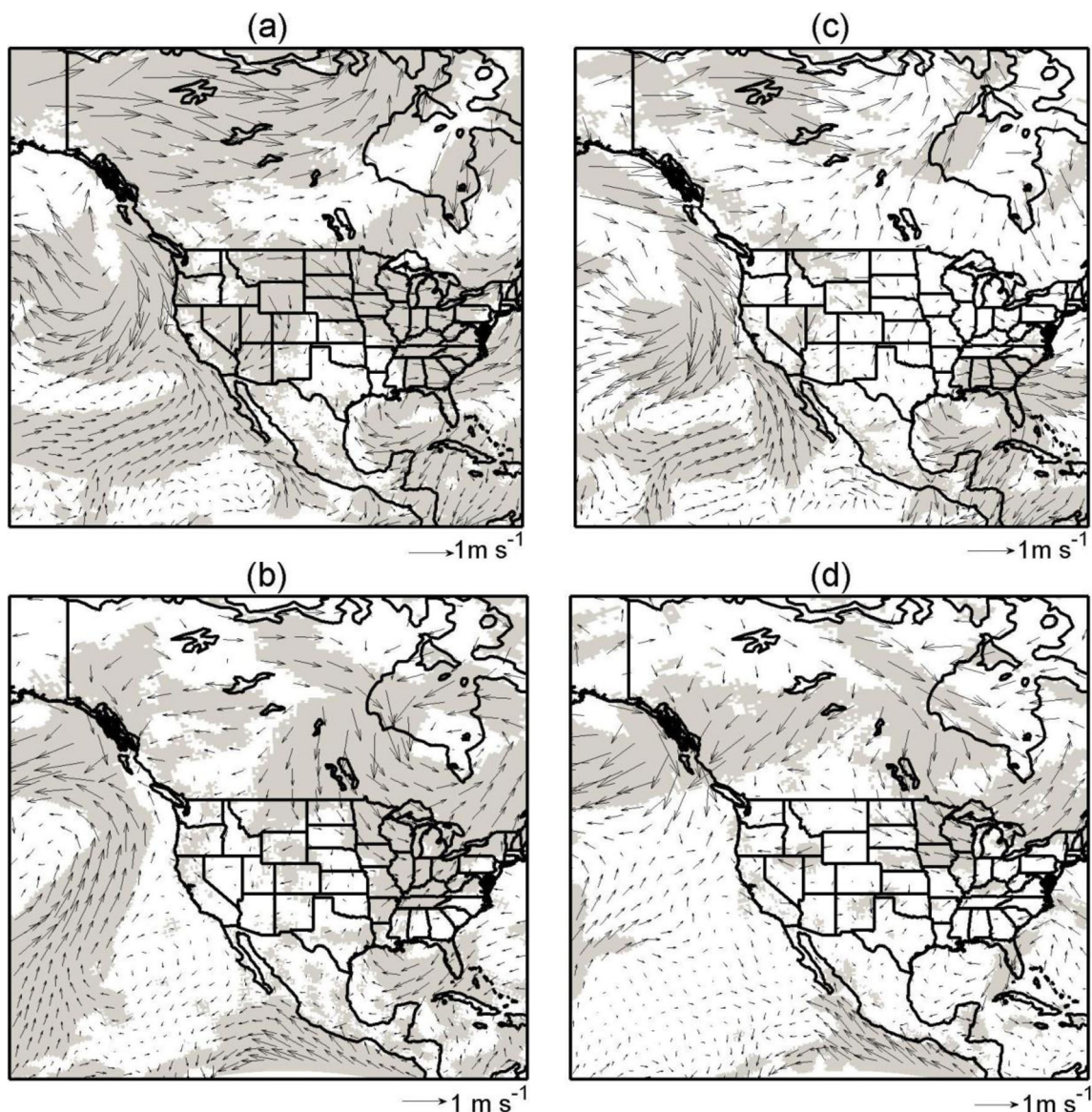


Fig. 7 The same as Fig. 4, but for 10-m wind anomalies (m s^{-1})

the western and central portions of the USA and much of Canada and the negative trend over the Gulf of Alaska (Fig. 3c).

3.2 EOF analysis

The EOF technique is applied to extract and rank the most common anomalous 500-hPa geopotential-height patterns associated with the 203 very large and the 80 extremely large wildfires, and the results are shown in Fig. 4. The first EOF mode explains 22.1% and 24.2% of the total variance in the

observed geopotential height anomaly patterns associated with the two fire-size categories, respectively. The second mode accounts for 17.7% and 19.1%, respectively. The corresponding near-surface atmospheric conditions are obtained through regressions of the anomalous surface temperatures, relative humidity, and wind onto the time series or the principal components (PC) of the two leading EOF modes; the results are shown in Figs. 5, 6, and 7.

The overall spatial patterns of the first EOF mode of the 500 hPa geopotential height anomalies are similar for the two

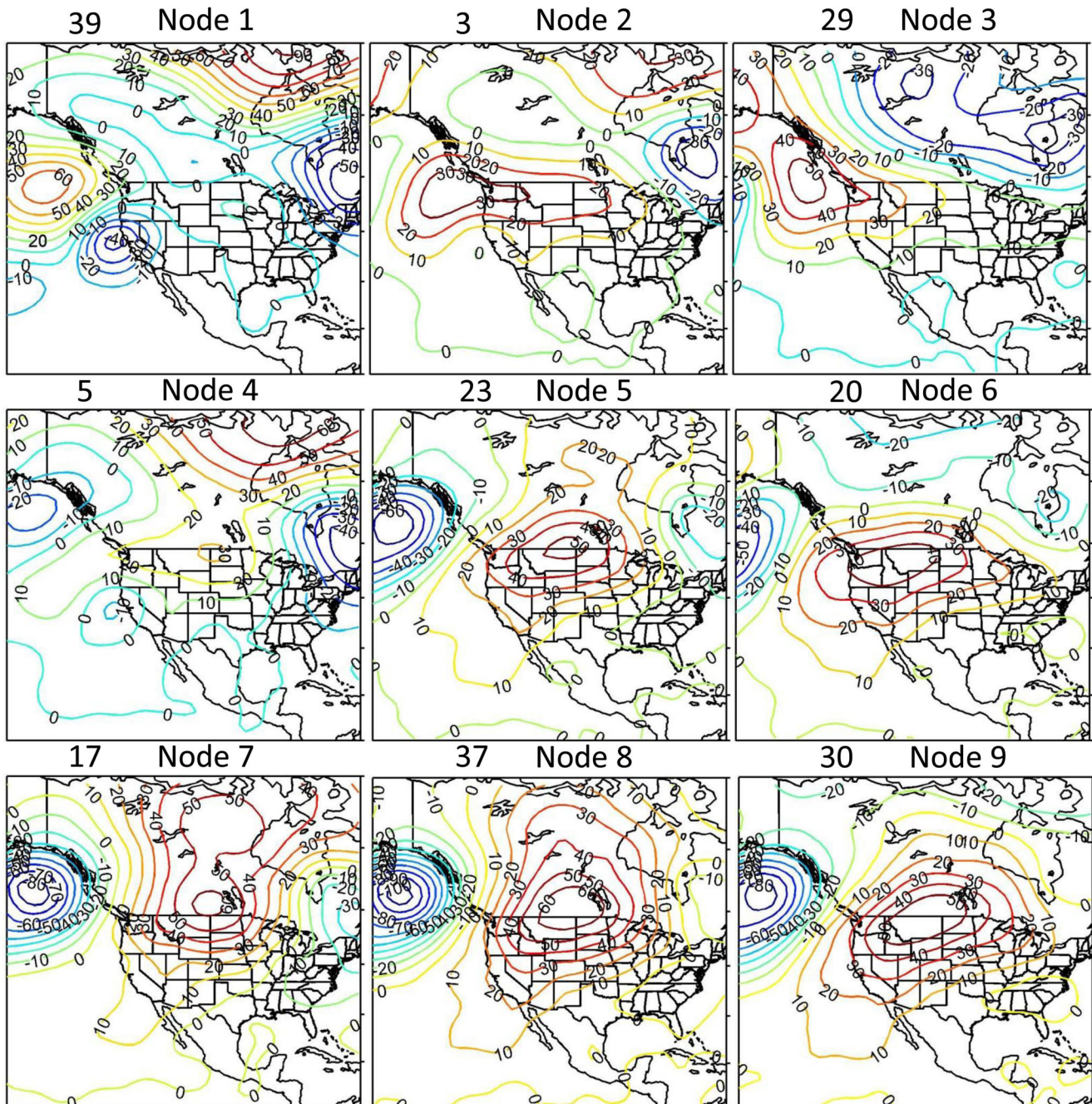


Fig. 8 The 3×3 SOM patterns of 500-hPa geopotential height anomalies (gpm) corresponding to very large wildfire events. The number at the top left of each panel indicates the number of occurrence of the pattern

fire-size categories. The patterns show positive geopotential height anomalies over much of the continental U.S., with maximum values centered over Pacific Coast and over the New England Coast. Meanwhile, negative geopotential height anomalies appear over northern and central Canada and over the Gulf of Alaska. Comparing the two fire-size categories, the anomalies (both positive and negative) for extremely large fires are stronger and the positive anomaly center moved northward from the New England Coast to Canada’s East Coast.

At the surface, the regression analyses suggest that the first EOF mode for the 500-hPa geopotential height anomalies for the two fire-size categories are associated with significant positive temperature anomalies over the Pacific Coast and western portions of the Intermountain regions, as well as over the northeastern U.S. (Fig. 5). Negative temperature anomalies are found over much of northern and central Canada and along the Gulf Coast of the U.S. Surface relative humidity anomaly patterns (Fig. 6) are fairly consistent with the temperature

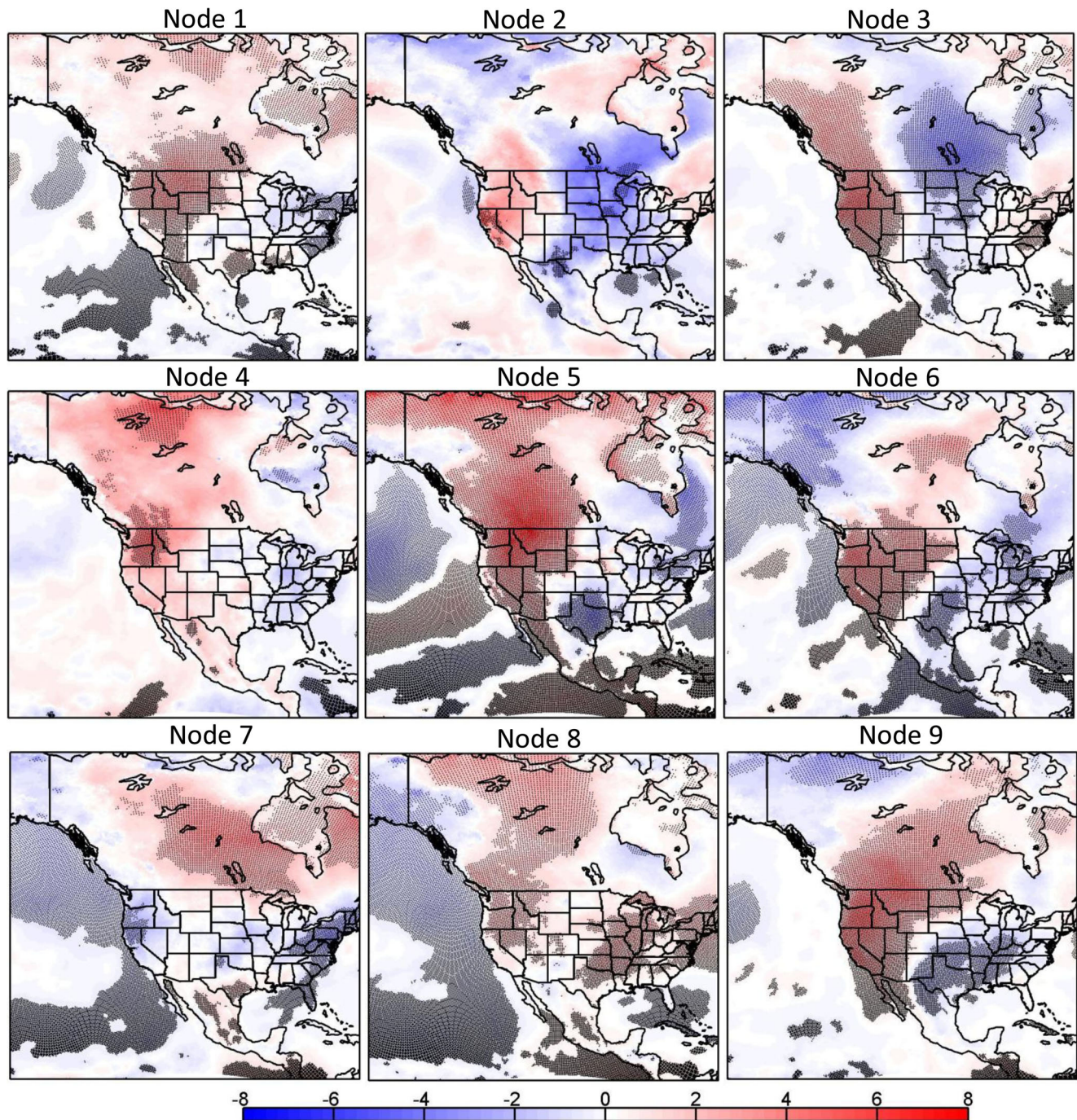


Fig. 9 Composite map of 2-m air temperature anomalies (°C) for each of the 9 SOM nodes in Fig. 8

anomaly patterns, with negative relative humidity anomalies generally occurring where positive temperature anomalies occur. An exception occurs over the northeastern U.S., where positive relative humidity anomalies occur at where positive temperature anomalies are present, an indication that relative humidity in the northeastern U.S. is not always dominated by temperature. The anomalous surface wind vector field for the first EOF mode is dominated by an anticyclonic cell off the Pacific coast of southwestern Canada and northwestern U.S.

(Fig. 7). Sinking motion and adiabatic warming and drying associated with the anomalous high along with warm and less humid conditions at the surface over the northwestern U.S. produce an environment prone to large wildfires.

Despite the similarity in the general patterns, some differences exist between the very large and the extremely large fires at both the surface and at the 500 hPa level. For extremely large fires, the negative geopotential height anomalies over the Gulf of Alaska are somewhat stronger

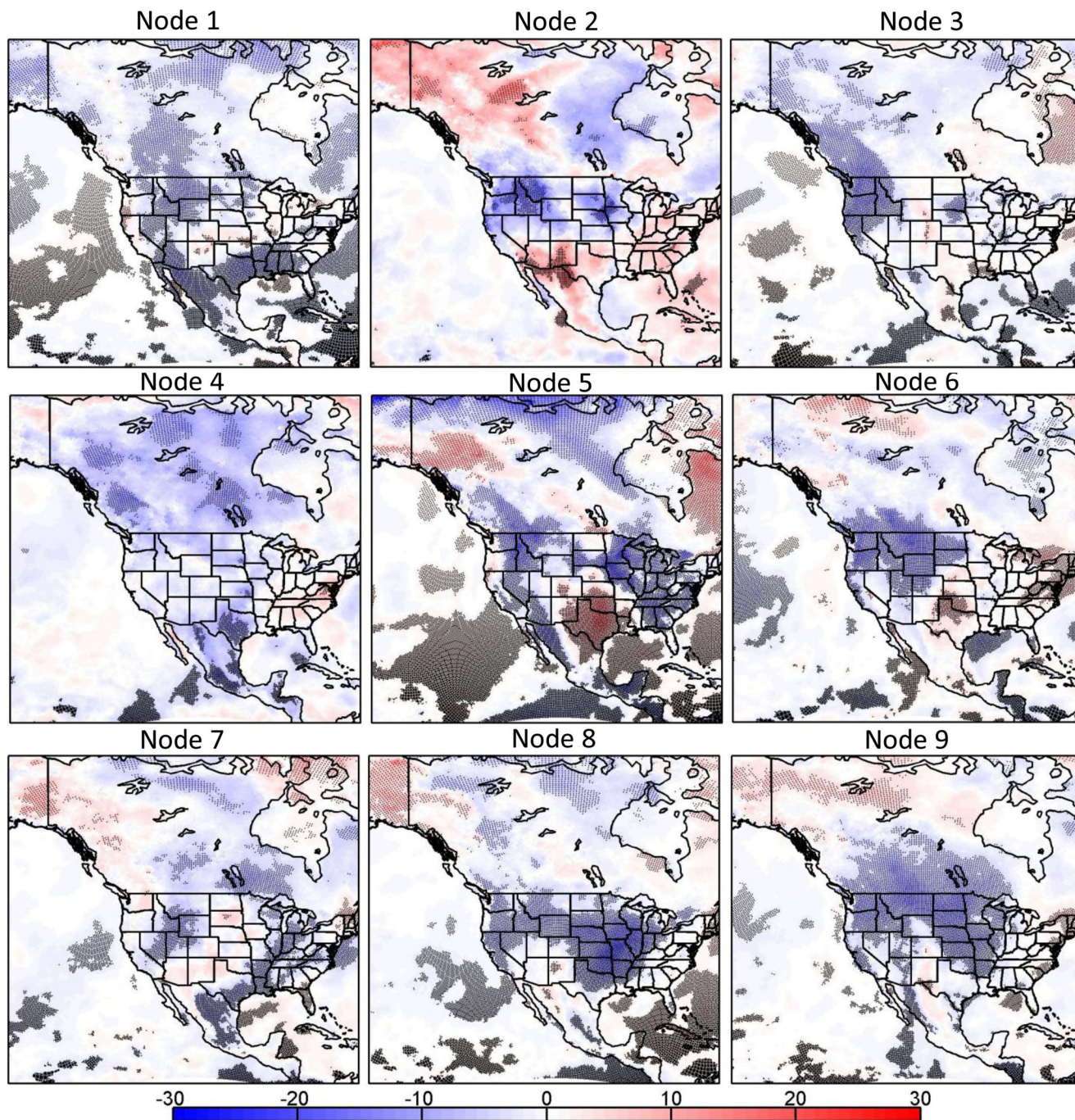


Fig. 10 The same as Fig. 9, but for 2-m relative humidity anomalies (%)

and the positive height anomalies along the West Coast are slightly stronger. Also, compared to the very large fire-size category, the extremely large fire-size category appears to be accompanied by weaker surface winds and positive surface temperature anomalies extending eastward across the Great Plains and the Midwest. These subtle differences in synoptic patterns are consistent with what would be expected for larger fires.

The second EOF modes for the two fire-size categories are dominated by negative 500-hPa geopotential height anomalies over much of Canada and positive anomalies over the Gulf of Alaska extending to the northwestern U.S. Anomalously warm, dry, and weak anti-cyclonic flows are found at the surface in the regions under the high. The major differences between the two fire-size categories are that the extremely large fires appear to be

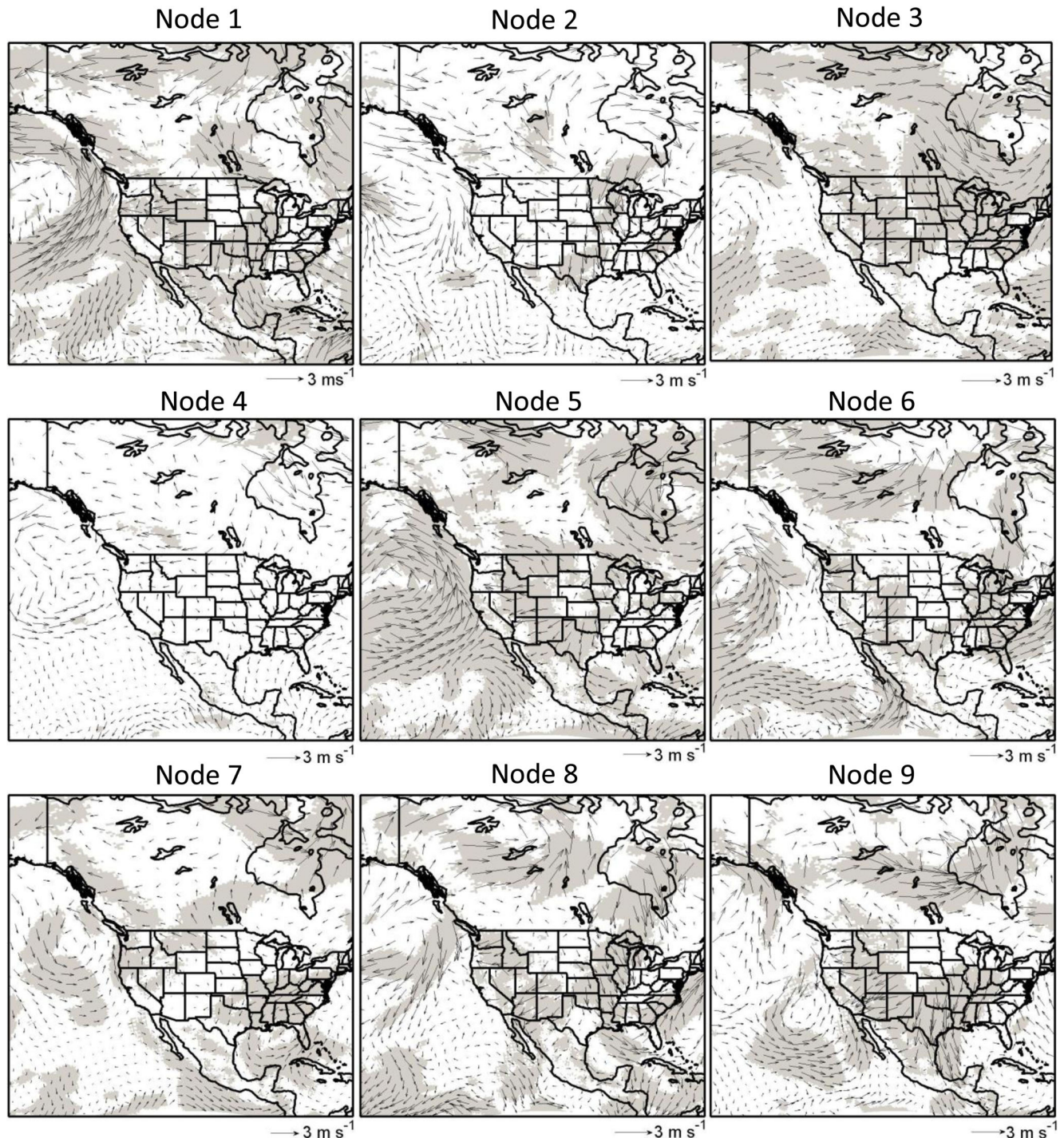


Fig. 11 The same as Fig. 9, but for 10-m wind anomalies (m s⁻¹)

associated with somewhat stronger negative geopotential height anomalies positioned further east in Canada and the positive height anomalies over the Gulf of Alaska extending farther inland into the western portions of the USA.

The EOF analyses allow for the identification of multiple key synoptic patterns associated with large wildfires as opposed to the Composite analyses that show only the average pattern.

3.3 SOM analysis

3.3.1 Very large fires

The variability of the anomalous 500 hPa geopotential height patterns corresponding to the 203 very large fires are depicted by a 3×3 SOM grid (Fig. 8). The 3×3 grid is chosen as the optimal grid for classifying synoptic patterns associated with very large wildfires in the study domain after testing larger

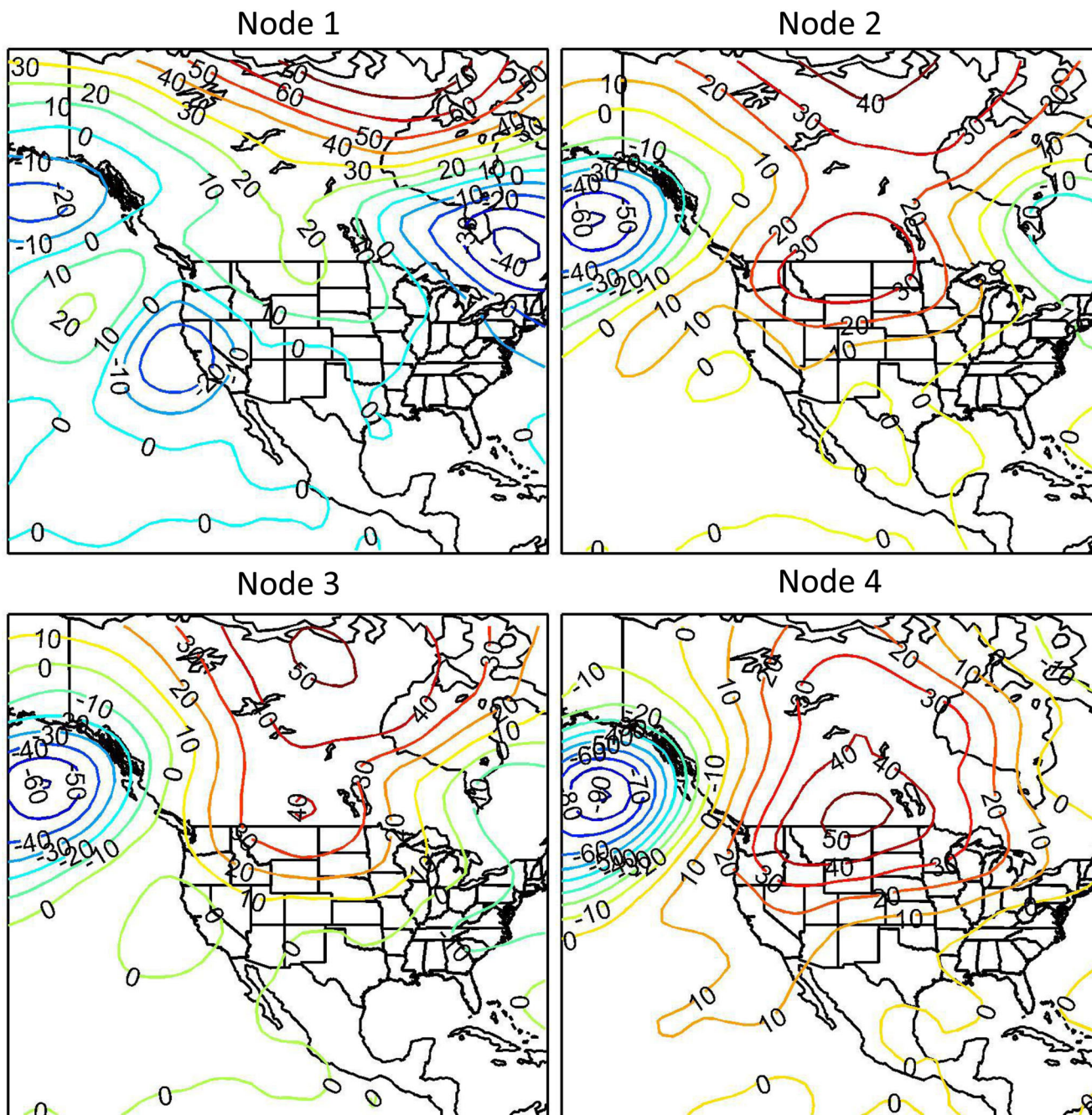


Fig. 12 The 2×2 SOM patterns of 500-hPa geopotential height anomalies (gpm) corresponding to extremely large wildfire events. The number at the top left of each panel indicates the number of occurrences of the pattern

(4×5) and smaller (2×2) grids. A larger grid produces more details, but makes interpretation more difficult, while a smaller grid overly generalizes the patterns.

Among the 9 nodes in the 3×3 grid, nodes 1 and 8 depict the synoptic patterns associated with 39 and 37 out of the 203 very large fires. Nodes 9 and 3 depict patterns associated with 30 and 29 of the very large fire events, respectively, while nodes 5 and 6 are associated with 23 and 20 of the very large fires, respectively. Node 7 is associated with 17 fires, and nodes 2 and 4 are associated with only a few events. The smaller magnitudes of the geopotential height anomalies and the weaker gradients for nodes 2 and 4, indicating smaller deviation from the averaging patterns, are consistent with the fewer cases.

Except for node 1 and to some degree node 4, the spatial patterns are quite similar, with large positive anomalies over

much of the western and central U.S. and southern Canada and large negative anomalies over the Gulf of Alaska. However, the position and strength of the anomalies vary among the nodes. This remarkable similarity in 7 out of the 9 SOM nodes indicates that a majority (159 out of 203, or approximately 78%) of the very large wildfires in the northwestern U.S. during the study period occurred under or just behind a synoptic ridge in the central and western U.S. ahead of a deep synoptic trough in the Gulf of Alaska. However, a fraction (28%) of the very large wildfires also occurred under the synoptic patterns represented by node 1 and node 4, where a weak trough exists over the Pacific Coast and a weak ridge exists over the north-central U.S.

Compared to the composite maps in Fig. 2, the dominant SOM spatial patterns represented by nodes 5 and 7–9 are

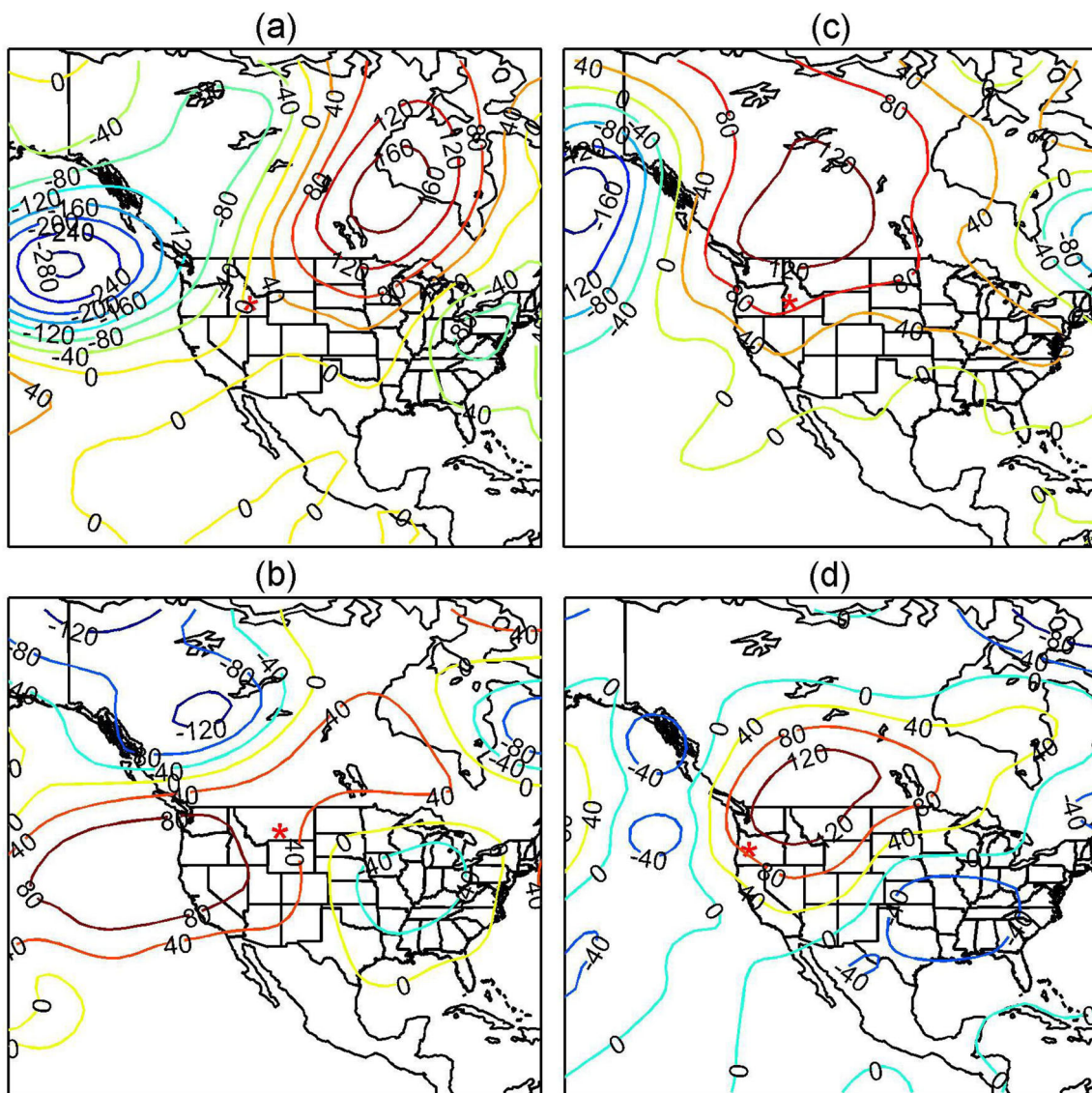


Fig. 13 Anomalous 500-hPa geopotential height (gpm) patterns for the occurrence of the four largest wildfires in the northwestern U.S. during the 1984–2014 period. Asterisks indicate the wildfire locations

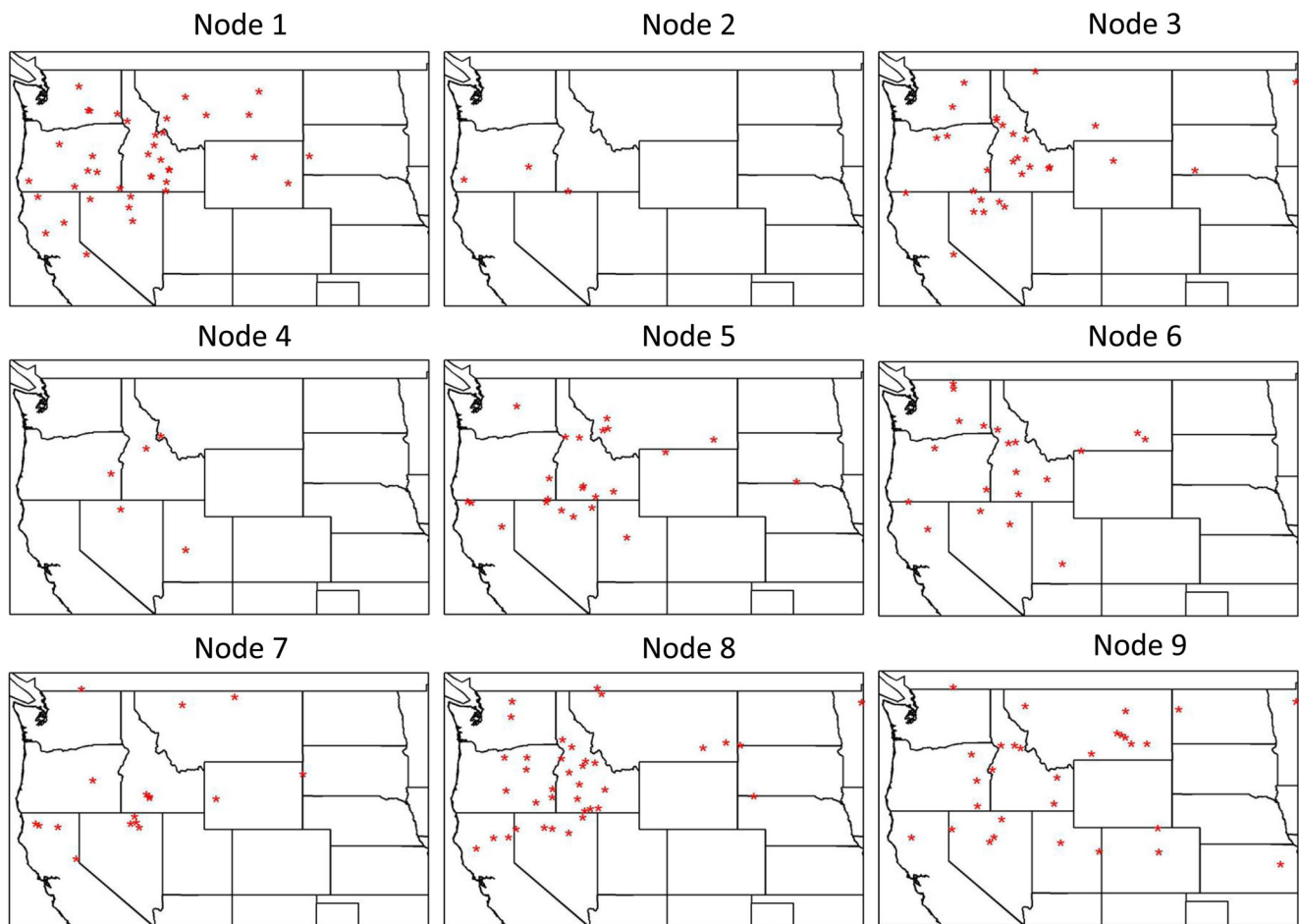


Fig. 14 Locations of the very large wildfires associated with each of the nine SOM nodes in Fig. 8

similar to the Composite pattern, especially the pattern depicted by node 5 that shows a close resemblance to the Composite map. While the Composite map is capable of portraying the dominant spatial pattern, it cannot depict the large differences in the strengths of the anomalies and the small differences in their positions as seen in the SOM patterns. Compared to the EOF patterns, the pattern of node 6, and to some degree of node 3, resemble the pattern of the first EOF mode, although there are some differences in the strength and locations of positive and negative anomaly centers. The percentage of the variance represented by the first EOF mode (22.1%) is similar to the combined percentage (24%) represented by node 6 (9.8%) and node 3 (14.2%). Interestingly, the pattern in the first EOF mode differs from the dominant SOM mode and the differences occur mostly in Canada where the first EOF mode depicts negative anomalies while the dominant SOM pattern displays positive anomalies. The pattern of node 1 bears some resemblance to that of the second EOF mode, and the percentage represented by node 1 (19.2%) is also similar to that of the second EOF mode (17.65%). A careful comparison reveals that the second EOF pattern represents more of a transitional state between node 1 and node 3.

Surface conditions corresponding to the anomalous 500-hPa height patterns represented by each SOM node are shown by the Composite maps (Figs. 9, 10, and 11). With the exception of node 7, the Composite maps show generally warmer (Fig. 9) and drier (Fig. 10) conditions over much of the western U.S., as easterly wind components around an anti-cyclonic cell (Fig. 11) transport continental air into the western U.S. as opposed to westerly winds transporting cooler air from the Pacific Coast. The variations in the strength and extent of the anti-cyclonic cell (Fig. 11) are consistent with the variation in the temperature (Fig. 9) and humidity (Fig. 10) among the nodes. For node 7, winds around the cyclonic cell off the Pacific Coast bring cooler and wetter conditions into the Northwest and northern California, but warmer and drier condition still prevails in the region of the Intermountain West where a majority of the very large wildfires occurred (Fig. 1).

3.3.2 Extremely large fires

A smaller (2×2) SOM grid is utilized to classify synoptic patterns for extremely large wildfires, and the results are shown in Fig. 12. Except for node 1, all nodes exhibit a blocking pattern with

positive height anomalies over the north central U.S. and southern Canada sandwiched by strong negative height anomalies over the Gulf of Alaska and weaker negative anomalies over southeastern Canada. This pattern is similar to the dominant pattern for very large fires (nodes 5, 7–9, Fig. 8). However, one node (node 1) representing 25 out of 80 (31%) of the cases shows a distinctly different pattern with a trough over the Pacific Coast, which is similar to node 4 and node 1 for the very large wildfire events (Fig. 8). Compared to the Composite and EOF methods, the Composite pattern (Fig. 2) is very similar to that in node 3. The first EOF pattern (Fig. 3) bears some resemblance to the dominant SOM patterns (depicted by nodes 4, 3, and 2), although the extent and strengths of the positive and negative anomalies in the first EOF mode differ from those of nodes 4, 3, and 2 in the SOM. None of the four nodes were similar to the second EOF pattern.

The composites of surface atmospheric variables corresponding to the 4 SOM nodes (not shown) show warmer and drier surface conditions in the Intermountain West where most of the extremely large fires occurred.

3.4 Individual cases

The anomalous 500-hPa geopotential height fields on the days when the four largest wildfires started during the study period are examined (Fig. 13). These four fires, with locations indicated in Fig. 13, occurred on 21 July 2007, 22 July 1988, 8 July 2012, and 13 July 2002, and burned 567,410; 565,099; 557,622; and 495,302 acres (229,623; 228,688; 225,662; and 200,442 ha), respectively, during the course of the fires. Although there are some differences in the synoptic patterns, all four fires occurred under an anomalous 500-hPa high. Three out of the four fires (first, third, and fourth) had a synoptic pattern identified by the Composite, the first EOF mode, and the dominant SOM nodes, although the positions of the anomalous ridge and trough and their strengths differ considerably. The pattern for the second largest fire closely resembles the second EOF mode and that of SOM node 2.

4 Discussion and conclusion

Three pattern classification methods, namely Composite, EOF, and SOM, were utilized to identify the synoptic patterns associated with the occurrences of very large ($\geq 50,000$ acres or 20, 250 ha) and extremely large ($\geq 100,000$ acres or 40,500 ha) wildfires in the northwestern U.S. during the period 1984–2014. All three methods indicate that for both fire-size categories, the dominant anomalous 500-hPa synoptic pattern is characterized by positive height anomalies over the western and central U.S. and central Canada flanked by negative anomalies over eastern Canada and the Gulf of Alaska. At the surface, the large wildfires are mainly associated with generally warmer and drier conditions as easterly

wind components around an anomalous anti-cyclonic cell over the Intermountain West bring interior continental air into the northwestern U.S. These results are in agreement with previous findings (e.g., Takle et al. 1994; Westerling et al. 2006; Crimmins 2006; Yu et al. 2013). Compared to very large fires, the extremely large fires are associated with more intense 500-hPa height anomalies that cover more extended regions and weaker surface winds.

The key circulation patterns identified here (Fig. 4a, c) are similar to that of the positive summertime North Atlantic Oscillation (NAO) index characterized by positive 500-hPa geopotential height anomalies over much of the contiguous U.S. and negative anomalies over northern Canada and the eastern North Pacific (<https://www.cpc.ncep.noaa.gov/products/precip/CWlink/pna/nao.loading.shtml>). Yu et al. (2013) also noted the connection of the positive summertime NAO and higher wildfire potentials as defined by higher Haines index values (in their Figs. 4 and 5).

Despite their different levels of complexity, all three methods are able to depict the basic synoptic pattern. As expected, the geopotential height anomaly patterns are smoother and weaker with the Composite methodology as a result of averaging patterns with small shifts in positions of the key features (ridges and troughs). Although the patterns from the leading EOF modes are comparable to some of the SOM nodes, the SOM methodology brings out the differences in the strengths and locations of the anomalies as well as other patterns representing transitions between synoptic regimes that can also be associated with fire events. The SOM analyses indicate that a portion (20–30%) of the large wildfires corresponded to a synoptic pattern that deviated from the basic pattern.

The utility of linking wildfires to their respective synoptic patterns using SOM classification can be illustrated by Fig. 14 that shows the locations of the very large wildfires related to each of the nine synoptic circulation patterns identified by the SOM nodes (Fig. 8). Nodes 3 and 9 correspond to nearly the same number of fires (29 and 30, respectively), but represent different circulation patterns, with node 3 characterized by an anomalous high centered off the coast of the Pacific Northwest, extending eastward to western Montana, whereas node 9 characterized by a large anomalous higher over much of the north and central U.S. (Fig. 8). The spatial distributions of the corresponding very large wildfires (Fig. 14) seem to suggest that more fires east of the northern Rockies tend to occur under the node 9 circulation pattern compared to that of node 3. A further examination of the surface conditions under the two synoptic weather patterns (Figs. 9, 10, and 11) reveals a warmer and drier environment east of the northern Rockies under node 9 compared to the environment under node 3. The ability to relate the differences in synoptic circulation patterns to the differences in fire clusters by the SOM classification method is limited here by the relatively small number of fires; the benefit will become more evident when more fires across a

larger region are used in the analysis. This information on possible fire-prone locations under each synoptic pattern can be very useful for resource allocation and fire management.

Previous studies (e.g., Schroeder 1969; Swetnam and Betancourt 1990; Westerling et al. 2003; Crimmins and Comrie 2004; Dixon et al. 2008; Mason et al. 2017) have indicated that wildfire regimes respond to atmospheric variability through low-frequency (seasonal and interannual) drought (or ample precipitation)–fuel feedback and high-frequency (daily, hourly) fluctuation of temperature, humidity, and wind. Synoptic circulation patterns effectively link both short- and long-term atmospheric variability, and thus, a classification of fire-prone synoptic circulation patterns, as obtained from this study for the northwestern U.S., can be an integral part of decision making tools for fire managers.

This study is limited to the identification of synoptic patterns and surface conditions associated with very large and extremely large wildfires in the northwestern U.S. Future studies, particular modeling studies, are needed to more fully understand how these patterns develop and evolve and how they contribute to regional and local atmospheric dynamics that are conducive to the spread of wildfires. Another caveat of this study is that the synoptic patterns identified correspond only to the beginning of the fire events. It would also be useful to identify synoptic patterns before and during periods of major fire spread for each wildfire event.

Acknowledgements Support for this research was provided by the USDA Forest Service via Research Joint Venture Agreement 16-JV-11242306-101. This work is also partially supported by the USDA National Institute of Food and Agriculture, Hatch project 1010691. We would like to acknowledge the source for the NARR data.

References

- Bessie WC, Johnson EA (1995) The relative importance of fuels and weather on fire behavior in Sub-Alpine forests. *Ecology* 76:747–762
- Brotak EA, Reifsnnyder WE (1977) An investigation of the synoptic situations associated with major wildland fires. *J Appl Meteorol* 16: 867–870
- Burgan RE, Andrews PL, Bradshaw LS, Chase CH, Hartford RA, Latham DJ (1997) WFAS: Wildland fire assessment system. *Fire Manag Notes* 57:14–17
- Crimmins MA (2006) Synoptic climatology of extreme fire-weather conditions across the Southwest United States. *Int J Climatol* 26:1001–1016
- Crimmins MA, Comrie AC (2004) Wildfire-climate interactions across Southeast Arizona. *Int J Wildland Fire* 13:455–466
- Dixon PG, Goodrich GB, Cooke WH (2008) Using teleconnections to predict wildfires in Mississippi. *Mon Weather Rev* 136:2804–2811
- Duane A, Brotons L (2018) Synoptic weather conditions and changing fire regimes in a Mediterranean environment. *Agri Fore Meteorol* 254:190–202
- Eidenshink J, Schwind B, Brewer K, Zhu Z, Quayle B, Howard S (2007) A project for monitoring trends in burn severity. *Fire Ecology* 3:3–21
- Flannigan MD, Wotton BM (2001) Climate, weather, and area burned. In: Johnson EA, Miyanishi K (eds) *Forest fires: behavior and ecological effects*. Academic Press, Cambridge, pp 351–373
- Hannachi A, Jolliffe IT, Stephenson DB (2007) Empirical orthogonal functions and related techniques in atmospheric science: a review. *Int J Climatol* 27:1119–1152
- Hayasaka H, Tanaka HL, Bieniek PA (2016) Synoptic-scale fire weather conditions in Alaska. *Polar Sci* 10:217–226
- Hewitson BC, Crane RG (2002) Self-organizing maps: applications to synoptic climatology. *Clim Res* 22:13–26
- Hong Y, Hsu K, Sorooshian S, Gao X (2005) Self-organizing nonlinear output (SONO): a neural network suitable for cloud patch-based rainfall estimation at small scales. *Water Resour Res* 41. <https://doi.org/10.1029/2004WR003142>
- Hsieh WW (2001) Non-linear principal component analysis by neural network. *Tellus* 53:599–615
- Janjic ZI (1994) The step-mountain Eta coordinate model: further developments of the convection, viscous sublayer, and turbulence closure schemes. *Mon Weather Rev* 122:927–945
- Kohonen T (1995) *Self-organizing maps*, 2nd edn. Springer, Berlin 501 pp
- Malmgren BA, Winter A (1999) Climate zonation in Puerto Rico based on principal components analysis and an artificial neural network. *J Clim* 12:977–985
- Mason SA, Hamlington PE, Hamlington BD, Jolly WM, Hoffman CM (2017) Effects of climate oscillations on wildfire potential in the Central United States. *Geophys Res Lett.* <https://doi.org/10.1002/2017GL074111>
- Mesinger F, DiMego G, Kalnay E, Mitchell K, Shafran PC, Ebisuzaki W, Jović D, Woollen J, Rogers E, Berbery EH, Ek MB, Fan Y, Grumbine R, Higgins W, Li H, Lin Y, Manikin G, Parrish D, Shi W (2006) North American regional reanalysis. *Bull Am Meteorol Soc* 87:343–360
- Monahan AH, Fyfe JC, Ambaum MHP, Stephenson DB, North GR (2009) Empirical orthogonal functions: the medium is the message. *J Clim* 22:6501–6514
- Naren A, Maity R (2018) Modeling of local sea level rise and its future projection under climate change using regional information through EOF analysis. *Theor Appl Clim* 134:1269–1285
- Newark M (1975) The relationship between forest fire occurrence and 500 mb ridging. *Atmos.* 13:26–33
- North G, Bell TL, Cahalan RF, Moeng FJ (1982) Sampling errors in the estimation of empirical orthogonal functions. *Mon Weather Rev* 110:699–706
- Paschalidou AK, Kassomenos PA (2016) What are the most fire-dangerous atmospheric circulations in the Eastern-Mediterranean? Analysis of the synoptic wildfire climatology. *Sci Total Environ* 539:536–545
- Pereira MG, Trigo RM, da Camara CC, Pereira JMC, Leite SM (2005) Synoptic patterns associated with large summer forest fires in Portugal. *Agri Fore Meteorol* 129:11–25
- Richman MB (1986) Rotation of principal components. *J Clim* 6:293–335
- Ruffault J, Moron V, Trigo RM, Curt T (2016) Daily synoptic conditions associated with large fire occurrences in Mediterranean France: evidence for a wind-driven fire regime. *Int J Climatol* 35:524–533
- Schroeder MJ (1969) *Critical fire weather patterns in the conterminous United States*. Office of Meteorological Operations, Silver Spring 31pp
- Sheridan SC, Lee CC (2011) The self-organizing map in synoptic climatological research. *Prog Phys Geogr* 35:109–119
- Simmons AJ, Branstator GW, Wallace JM (1983) Barotropic wave propagation, instability and atmospheric teleconnection patterns. *J Atmos Sci* 40:1363–1392
- Swetnam TW, Betancourt JL (1990) Fire-Southern oscillation relations in the southwestern United States. *Science* 249:1017–1020

- Takle ES, Bramer DJ, Heilman WE, Thompson MR (1994) A synoptic climatology for forest fires in the NE US and future implications from GCM simulations. *Int J Wildland Fire* 4:217–224
- Trouet V, Taylor AH, Carleton AM, Skinner CN (2009) Interannual variation in fire weather, fire extent, and synoptic scale circulation patterns in northern California and Oregon. *Theor Appl Clim* 95: 349–360
- Wang T, Franz TE, Li R, You J, Shulski MD, Chittaranjan R (2017) Valuating climate and soil effects on regional soil moisture spatial variability using EOFs. *Water Resour Res* 53:4022–4035
- Westerling AL, Brown TJ, Gershunov A, Cayan DR, Dettinger MD (2003) Climate and wildfire in the Western United States. *Bull Am Meteorol Soc* 84:595–604
- Westerling AL, Hidalgo GH, Cayan DR, Swetnam TW (2006) Warming and earlier spring increase western US forest wildfire activity. *Science* 313:940–943
- Yu L, Zhong S, Bian X, Heilman WE, Charney JJ (2013) The interannual variability of the Haines Index over North America. *J Appl Meteorol Climatol* 52:2396–2409
- Yu L, Zhong S, Zhou M, Sun B, Lenschow DH (2018) Antarctic summer sea ice trends in the context of high latitude atmospheric circulation changes. *J Clim* 31:3909–3920

Publisher's note Springer Nature remains neutral with regard to jurisdictional claims in published maps and institutional affiliations.